Available online at www.sciencedirect.com
ScienceDirect
Phytochemistry 68 (2007) 2197–2210
PHYTOCHEMISTRY
www.elsevier.com/locate/phytochem

Compartment-specific labeling information in ^{13}C metabolic flux analysis of plants

Doug K. Allen *, Yair Shachar-Hill, John B. Ohlrogge

Department of Plant Biology, Michigan State University, East Lansing, MI 48824, USA

Received 15 January 2007; received in revised form 4 April 2007
Available online 25 May 2007

Abstract

Metabolic engineering of plants has great potential for the low cost production of chemical feedstocks and novel compounds, but to take full advantage of this potential a better understanding of plant central carbon metabolism is needed. Flux studies define the cellular phenotype of living systems and can facilitate rational metabolic engineering. However the measurements usually made in these analyses are often not sufficient to reliably determine many fluxes that are distributed between different subcellular compartments of eukaryotic cells. We have begun to address this shortcoming by increasing the number and quality of measurements that provide ^{13}C labeling information from specific compartments within the plant cell. The analysis of fatty acid groups, cell wall components, protein glycans, and starch, using both gas chromatography/mass spectrometry and nuclear magnetic resonance spectroscopy are presented here. Fatty acid labeling determinations are sometimes highly convoluted. Derivatization to butyl amides reduces the errors in isotopomer resolution and quantification, resulting in better determination of fluxes into seed lipid reserves, including both plastidic and cytosolic reactions. While cell walls can account for a third or more of biomass in many seeds, no quantitative cell wall labeling measurements have been reported for plant flux analysis. Hydrolyzing cell wall and derivatizing sugars to the alditol acetates, provides novel labeling information and thereby can improve identification of flux through upper glycolytic intermediates of the cytosol. These strategies improve the quantification of key carbon fluxes in the compartmentalized flux network of plant cells.

Keywords: Subcellular compartmentation; ^{13}C MFA; Stable isotope tracer; Soybean; Cell wall; Protein glycans; Starch; Glycerolipids; Oilseed; GC–MS; NMR

1. Introduction

The cellular functions and phenotypes of biological systems are closely related to the fluxome (Klapa et al., 2003), which is a measure of an organism's vitality. In recent years powerful labeling strategies and mathematical tools have been developed that allow the simultaneous determination of hundreds of *in vivo* metabolic fluxes in microorganisms. Most large scale flux analyses are based on steady-state approaches, and it is with these that we are concerned here, although kinetic approaches have also been used (see reviews by Morgan and Rhodes, 2002; Ratcliffe and Shachar-Hill, 2006).

In the early 1990s, fluxome studies were reported for bacteria (Varma et al., 1993a,b). Using linear programming and the assumption that a cell is maximizing a particular function (such as growth) it has been possible to use a limited number of measurements to calculate net metabolic fluxes, although the extent of reversibility of these steps remained largely unknown. These studies involved mass balancing of all of the metabolite pools (influxes equaling effluxes for each metabolite) in the metabolic network being considered. More details on this approach, known as flux balance analysis (FBA), and the underlying assumptions on which it depends are described by Aiba and Matsuoka (1979), Varma et al. (1993a,b), van der Heijden et al.

* Corresponding author. Tel.: +1 517 432 7120; fax: +1 517 353 1926.
E-mail address: allendo5@msu.edu (D.K. Allen).

0031-9422/$ - see front matter © 2007 Elsevier Ltd. All rights reserved.
doi:10.1016/j.phytochem.2007.04.010

(1994), and Stephanopoulos et al. (1998). More recently the use of defined labeled media and spectroscopic analysis of stable isotopic labeling patterns (Szyperski, 1995, 1998; Hellerstein and Neese, 1999) has permitted network-based balancing of isotopomers (variants of the same molecule containing different patterns of isotopic labeling) (Zupke and Stephanopoulos, 1994; Schmidt et al., 1997; Wittmann and Heinzle, 1999) and has allowed the determination of reversible as well as net metabolic fluxes (Follstad and Stephanopoulos, 1998; van Winden et al., 2005). Specialized algorithms, software, and statistical evaluation tools have been applied for these analyses (e.g. Wiechert et al., 2001; Zamboni et al., 2005; Antoniewicz et al., 2007; Libourel et al., 2007).

The existence of such tools opened the door for fluxomic studies of plants, but these have been relatively few in number, mostly for two reasons. First, plant primary metabolism is highly compartmentalized with multiple discrete metabolite pools, and the same biochemical reactions often occur in different organelles, increasing the challenges facing analyses of these eukaryotic metabolic networks (Fig. 1). Second, such investigations require an unusual combination of computational/theoretical skills together with experience in experimental plant metabolic biochemistry as well as MS and/or NMR expertise. Nevertheless, metabolic flux analysis based on steady-state isotopic labeling of plants has now been carried out by culturing plants, cells or tissues in defined media under conditions of metabolic pseudo-steady state (Rontein et al., 2002; Schwender et al., 2003, 2004, 2006; Sriram et al., 2004; Alonso et al., 2005; Ettenhuber et al., 2005, 2006; Spielbauer et al., 2006). The theory and practice of this subject as it pertains to plants was reviewed by Ratcliffe and Shachar-Hill (2006) and some of the most recent progress is described in other articles in this journal issue.

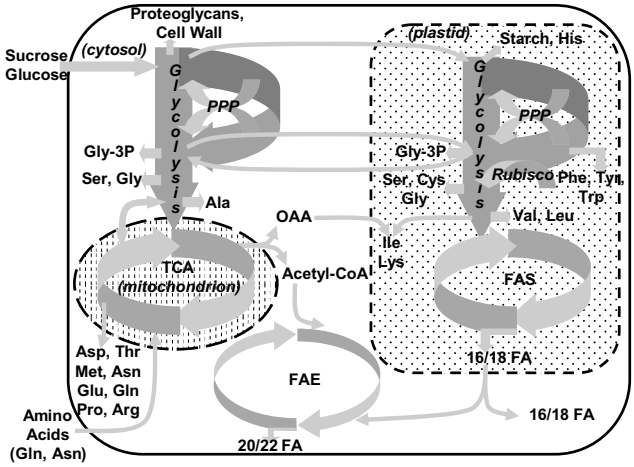

Fig. 1. Illustration of plant central metabolism in heterotrophic and autoheterotrophic cells, showing the processes supporting the synthesis of fatty acids, carbohydrates and amino acids. The complexities that make flux analysis challenging include the partitioning of metabolism into three major compartments, and the duplication of many intermediates and some pathways between them. Omissions include the assimilation of amino acids into protein and the synthesis of some amino acids in additional subcellular compartments. *Abbreviations*: PPP, pentose phosphate pathway; TCA, tricarboxylic acid cycle; FAS, fatty acid synthesis; FAE, fatty acid elongation; FA, fatty acid; His, histidine; Phe, phenylalanine; Tyr, tyrosine; Trp, tryptophan; Ile, isoleucine; Lys, lysine; Ser, serine; Cys, cysteine; Gly, glycine; Val, valine; Leu, leucine; Ala, alanine; Asp, aspartate; Thr, threonine; Met, methionine; Asn, asparagine; Glu, glutamate; Gln, glutamine; Pro, proline; Arg, arginine; Gly-3P, glycerol-3-phosphate.

In most studies isotopically-labeled carbon or nitrogen sources are provided to cell or tissue cultures and fluxes are established by a combination of biomass and label measurements. The contribution of different measurements to flux determination depends on their compartmental localization as well as their role in various metabolic pathways. While NMR and GC–MS measurement methods for labeling of proteinaceous amino acids are well established (Szyperski, 1995; Dauner and Sauer, 2000) there remain uncertainties about the subcellular location of the biosynthesis of some amino acids in plants (Lange and Ghassemian, 2005). Cell wall and protein glycan monomers are formed from nucleotide sugars that has well documented origins in the cytoplasm (Feingold and Avigad, 1980; Coates et al., 1980, Walter-Heldt, 2005), as does the acetyl-CoA used for fatty acid elongation beyond lengths of 18 carbons (Bao et al., 1998). In contrast, acetyl-CoA for *de novo* fatty acid synthesis is produced by plastidic pyruvate dehydrogenase (Bao et al., 2000) and plastidic starch biosynthetic enzymes are responsible for starch accumulation (Smith and Martin, 1993; daSilva et al., 1997). Accurate quantification of labeling in these storage metabolites can improve compartment-specific information and thereby improve fluxome analysis. In this study we describe methods that increase the available information on labeling patterns of biomass precursors and the application of these methods to metabolism in soybean seeds during filling.

2. Results and discussion

In the following sections we describe (1) a method to increase reliability of analysis of labeling in the acetyl building blocks of fatty acids; (2) the exploitation of this approach to provide compartmental information on acetyl groups consumed in plastidic fatty acid biosynthesis versus those used for fatty acid elongation in the cytosol; (3) a method to obtain improved ^{13}C positional enrichment and increased bond connectivity information from NMR spectra of starch glucose units; and (4) novel mass spectrometric measurements of labeling in cell wall, protein glycan, and starch glucose moieties that describe biomass fluxes from the cytosol or plastid into those pools.

2.1. Butyl amide fatty acid derivatives yield improved GC–MS spectra

The electron bombardment of volatilized fatty acid methyl esters (FAME) is characterized by the well-studied

McLafferty rearrangement that results in the generation of a series of ions differing in mass by increments of CH_2 (e.g. McLafferty, 1959; Ryhage and Stenhange, 1963; Takayama, 1995; Fagerquist and Schwarz, 1998). The two major fragment ions contain two and three carbons derived from the carboxyl end of fatty acid molecules and weigh 74 and 87 atomic mass units (amu's), respectively (Fig. 2). These two fragments contain the labeling profile of the repeating acetyl groups that are polymerized during fatty acid biosynthesis.

Obtaining accurate isotope labeling data from the C2 and C3 fragment ions of FAMEs is challenging for two reasons. First, gas phase hydrogen exchanges during electron bombardment can alter the apparent isotope ratios in ways that vary with instrumental conditions and from sample to sample (Tulloch and Hogge, 1985; Patterson and Wolfe, 1993; Fagerquist et al., 1999, 2001). Second, FAME mass spectra contain significant levels of interfering signals in both the 74 and 87 molecular weight regions due to the production of other fatty acid cleavage products (Fig. 2). As an example, a C_5H_9 alkyl fatty acid fragmentation product gives a signal at 69 amu (McLafferty, 1959). In a carbon labeling experiment where fatty acids become highly labeled, the $[M+5]^+$ mass isotopomer of this C_5H_9 alkyl fragment can significantly distort the mass isotopomer distribution of the C2 fragment ion at 74 amu. Thus the convoluted overlapping signals of breakdown products complicate the accurate quantification of labeling in the C2 McLafferty fragment of FAMEs. A further complication in analysis of FAME spectra is that unsaturated methyl esters give very different spectra than their saturated counterparts (Christie, 2003). The interruption in the acyl chain created by the double bonds and their subsequent migration during molecular ion formation in the mass spectrometer results in a range of intermediate products with more complex fragmentation patterns. Consequently, for unsaturated lipids the C2 fragment is frequently not the largest peak (e.g. see Supplementary materials Fig. S3). Previously we have used hydrogenation of unsaturated fatty acids to increase the reliability of analysis for these structures. Below we show that butyl amide derivatives of fatty acids can be used to circumvent the need for hydrogenation and to improve the accuracy of analysis without additional corrections previously advocated.

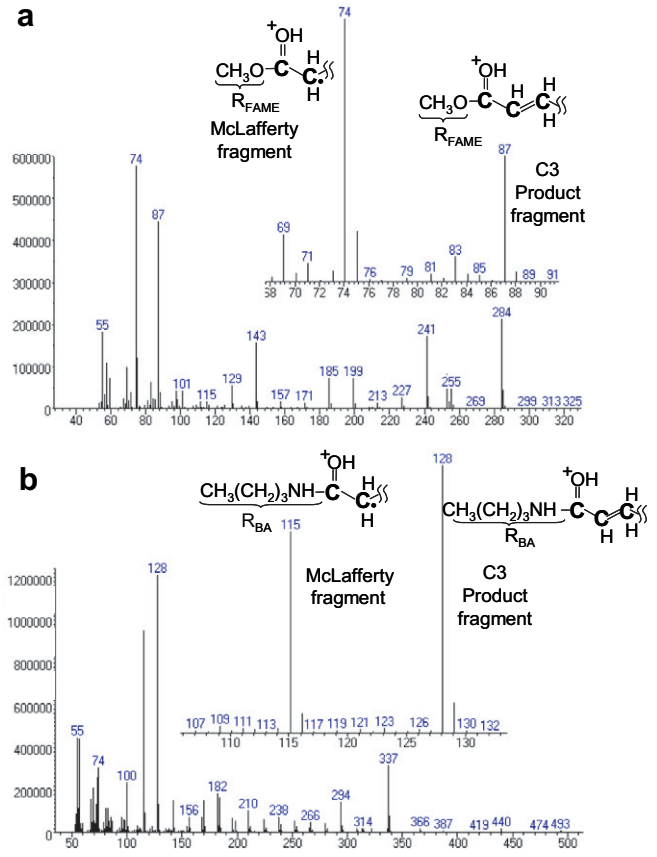

Fig. 2. (a) Mass spectrum of the FAME of 16:0 (16 carbon chain length fatty acid with no double bonds) with an inset of the region containing the C2 and C3 fragment signals that was acquired in selective ion monitoring mode. (b) Mass spectrum of the butyl amide derivative of an 18:1 fatty acid with an inset of the region containing the C2 and C3 fragment signals that was acquired in selective ion monitoring mode. Both (a) and (b) contain drawings of the C2 and C3 carbon fragments whose signals are used to measure labeling levels. The carbon atoms from the fatty acid in each fragment are shown in boldface type.

Butyl amide derivatives have previously been used to investigate alkyl-thioester composition and pool levels (acyl-ACP and acyl-CoA) in spinach (Kopka et al., 1995). Thioester-linked acyl chains react with *n*-butylamine via aminolysis with 90% yield in aqueous solution. We focused here on the reaction of *n*-butylamine with triacylglycerol. To react these nonpolar starting materials, hexane and pyridine were tested as the co-solvents of *n*-butylamine. For both solvent choices 4 M HCl was added at 48 h to stop the reaction and phase separate the products from unreacted compounds. Quantification of products in the nonpolar phase via integration of the GC peaks showed a sevenfold higher yield for the reaction performed in hexane. To ensure that products were quantitatively isolated, the polar phase was extracted twice more with 2 ml hexane and each aliquot was individually evaluated by TLC. On a mass basis the first extraction from the reaction performed in hexane demonstrated over 88% conversion to the butyl amide product and subsequent extractions indicate that the reaction approached completion (densitometric analysis of TLC plates not shown).

The intensities of specific mass peaks after correction for natural abundance are shown in Fig. 3 for both butyl amide and FAME derivatives. For butyl amide derivatives nearly all the signal intensity is associated with the $[M]^+$ unlabeled weight, which should represent 100% after correction for natural abundance (see the "standard" bars in Fig. 3). The FAME spectra do not correct well (average apparent ^{13}C labeling of 7%) because of increased $[M+1]^+$ signals that may reflect proton abstraction/transfer events (Fagerquist et al., 1999) or possibly contaminating ions from alkyl fragments of the FAME molecules. The $[M]^+$ fraction accounts for only ~85% of the total after correction for natural isotope abundances as opposed to a theoretical value of

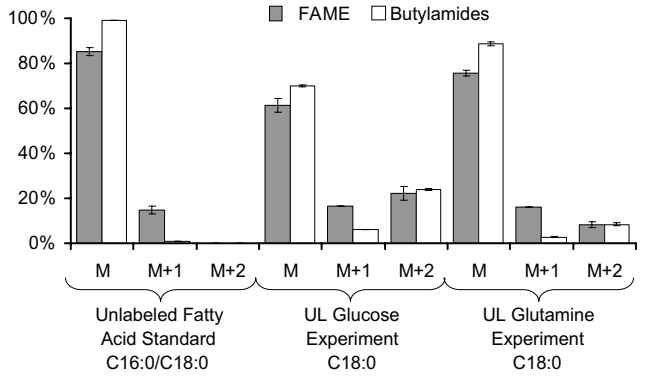

Fig. 3. Comparison of MS signal intensities from unlabeled standards (stearic and palmitic) and from labeled experimental samples (stearic) for the C2 fragments from FAME and butyl amide derivatizatives. Results shown are corrected for natural abundance. Unlabeled standards should correct to 100% $[M]^+$ with no other significant signals. Differences in the results for the two derivatives are significant for both $[M+1]^+$ and $[M+2]^+$ peaks. The erroneously large $[M+1]^+$ and low $[M]^+$ peaks in FAME spectra of unlabeled standards appear to contribute to increased $[M+1]^+$/reduced $[M]^+$ peaks in both labeling experiments as well.

100%. Preparation of the butyl amide derivative shifts the C2 fragment to a cleaner region in the mass spectrum and thus greatly reduces potential overlap. The butyl amide approach also produces fragments that are less prone to complications due to proton promiscuity, and as noted above particularly improves analysis of unsaturated acyl chains. It should be stated that the $[M-1]^+$ signal as a percentage of total signal (i.e. sum of $[M]^+$, $[M+1]^+$, $[M+2]^+$) was found to be small for both FAME (~4%) and butyl amide (~1%) standards suggesting that the protium loss is not the primary cause for poor correction.

We next analyzed the butyl amide and FAME derivatives of triacylglycerol produced by soybean embryos cultured in the presence of either 20% uniformly labeled hexose, [U-$^{13}C_6$]glucose or 100% uniformly labeled glutamine, [U-$^{13}C_5$]glutamine. Analysis of mass spectra of both the C2 and C3 fragments yields more than enough information to determine the labeling in odd and even numbered carbon positions of the fatty acids. The use of this redundant information also allows an internal check on the consistency of labeling information (a diagrammatic explanation is presented in the supplement).

Comparison of the peak intensities in mass spectra of FAME and butyl amide derivatives of labeled triacylglycerol from soybean embryos (Fig. 3) show distinct differences. Not surprisingly, the FAMEs that gave enhanced $[M+1]^+$ peaks in unlabeled standards show similar tendencies for the culture experiments relative to the butyl amides. This error is manifested in Table 1 (see boldface) where positional enrichments have been calculated from the mass weight profiles. Positional enrichment reflects fatty acid synthesis where the chain is successively extended by additional acetyl-CoA groups. Therefore the labeling in the even numbered carbon positions along the fatty acid chain must be equivalent, and likewise for the odd-numbered positions (i.e. enrichment of carbon 1 equals enrichment at carbons 3, 5, etc.). Using this, the spectra of butyl amides show nearly equivalent labeling in both acetyl-CoA carbons (i.e. position 1 versus position 2 of each acetyl-CoA unit); FAME spectra indicate a much larger enrichment in position 2 than 1. The disparity in positional labeling for FAMEs reflect the misleading high values of $[M+1]^+$ and low $[M]^+$ obtained by GC–MS analysis. Seven probability equations for the mass isotopomers of the two fragments (i.e. $[M]^+$, $[M+1]^+$, $[M+2]^+$ for the two carbon product, $[M]^+$, $[M+1]^+$, $[M+2]^+$, $[M+3]^+$ for the three carbon product), were used to derive the positional enrichment of the acetyl-CoA moiety with two carbon atoms. Assuming the same isotopomer distribution in the acetyl-CoA moieties and no isotope discrimination effects in FA chain elongation, the four unknowns representing the $2^n = 4$ isotopomers were resolved. A least square fit

Table 1
Comparison of fatty acid positional labeling measurements using FAME and butyl amide derivatives

Fatty acid chain	Labeling expt.	Derivatization method	Carbon enrichment	
			Position 1	Position 2
16 Carbons	[U-^{13}C]glucose	Butyl amide	26.6(<1)	26.2(<1)
		FAME	**21.2(3.6)**	**34.3(3.5)**
	[U-^{13}C]glutamine	Butyl amide	9.7(<1)	7.3(<1)
		FAME	**5.3(<1)**	**17.2(<1)**
18 Carbons	[U-^{13}C]glucose	Butyl amide	27.4(<1)	25.5(<1)
		FAME	**20.7(3.4)**	**35.5(3.3)**
	[U-^{13}C]glutamine	Butyl amide	10.4(1.1)	9.3(1.1)
		FAME	**6.0(1.0)**	**19.2(1.0)**
22 Carbons	[U-^{13}C]glucose	Butyl amide	22.6(1.3)	23.2(1.5)
	[U-^{13}C]glutamine	Butyl amide	27.5(<1)	29.9(<1)

Enrichments in cytosolically elongated fatty acids (containing 22 carbons) versus plastid-derived ones (c16 and c18) are shown for two labeling experiments (standard deviations are given in parenthesis). Position 1 and Position 2 refer to the carboxy-terminal carbons 1 and 2 of the fatty acid, derived from acetyl-CoA precursor. NMR of the triacylglyceride fraction from which the fatty acid derivatives were made (data not shown) confirms that the positional enrichments obtained from GC–MS of the butyl amide are correct (see text) by examining the acetyl-CoA of the fatty acid terminal methyl and $\omega - 1$ methylene carbons. For emphasis the inaccurate FAME results are in boldface type.

approach was applied to use redundant information in the data set, increasing the accuracy of the result. Calculated positional enrichments and standard deviations (from sensitivity analysis and error propagation) are given in parentheses in Table 1.

From the two labeling experiments described above, we also analyzed the labeled soybean triacylglycerol by one-dimensional ^{1}H and ^{13}C NMR (at 500 and 125 MHz, respectively, see Table 1). The absolute labeling in the terminal methyl group of soybean oil from the labeling experiments was calculated by peak integration to be 26.2% and 9.7% for the [U-^{13}C]glucose and [U-^{13}C]glutamine experiments, respectively. This serves as an independent measurement of the positional enrichments of carbon two in the acetyl-CoA group calculated in Table 1. Notably these numbers agree well with the butyl amide calculations for positional enrichment but not the FAME generated numbers (see Table 1). The ^{1}H signal of the methylene group adjacent to the terminal methyl group was too convoluted to determine absolute labeling from the proton NMR spectrum, however using ^{13}C NMR the labeling in the last two positions of the fatty acid were 95% and 98% equivalent for the [U-^{13}C]glucose and [U-^{13}C]glutamine experiments (data not shown) confirming that the positional enrichment was very similar in both positions of the acetyl-CoA unit consistent with the GC–MS-based calculation of positional enrichments from butyl amides given in Table 1. It is worth noting that the FAME mass spectra give dissimilar enrichments between positions, which conflicts with the NMR results. Taken together the NMR results strongly support the use of the butyl amide approach over FAME derivatization.

2.2. Cytosolic and plastidic pools of acetyl-CoA in soybean can be distinguished by butyl amide analysis

C16 and C18 (long-chain) fatty acids are synthesized in the plastid by fatty acid synthase. Following export of the fatty acids from the plastid to the cytosol a portion of these acyl chains are elongated by successive addition of two carbon units to create 20 carbon and longer fatty acids (very long-chain fatty acids). Consequently, the carboxy-terminal carbons of very long-chain fatty acids reflect the labeling of cytosolic acetyl-CoA, whereas the same carbons of C18 and shorter chain length fatty acids reflect label in the plastidic acetyl-CoA precursor. In studies of *B. napus* embryo metabolism, (Schwender and Ohlrogge, 2002; Schwender et al., 2006) used the abundant long-chain fatty acids in the oil to distinguish plastidic and cytosolic pools of acetyl-CoA. In contrast to *B. napus* where very long-chain fatty acids constitute more than 50% of acyl chains, C20 and C22 fatty acids are very minor components (<1%) of most plant oils. However, as described here the very high sensitivity of GC–MS detection allows labeling patterns in 20 and 22 carbon fatty acids from soybean embryos to be quantified, thereby providing compartmentally distinct metabolic flux information.

Analysis of soybean embryos labeled with [U-$^{13}C_6$]glucose or [U-$^{13}C_5$]glutamine revealed substantial differences in the labeling patterns for cytosolic and plastidic acetyl-CoA. In the glutamine experiment the average labeling in the cytosolic acetyl-CoA pool is three to four times higher than in the plastid reflecting the greater contribution of this amino acid to acetyl-CoA in the cytosol (Fig. 4). This can be seen in the mass intensities of C2 and C3 fragments which show a decreased degree of labeling in plastid-derived carbon. This observation is qualitatively consistent with our previous report on *B. napus* seeds (Schwender and Ohlrogge, 2002). Analysis of the glucose labeling experiment also supports the increased role of glutamine carbon to cytosolic acetyl-CoA over the plastidic form because the provision of a labeled glucose source results in higher labeling for the plastidic fragments with cytosolic fractions diluted by the unlabeled glutamine.

In vitro assays of fatty acid elongation by pea microsomes indicated that palmitate (C16) can be elongated by a cytosolic membrane-associated elongase (Bolton and Harwood, 1977; Barrett and Harwood, 1998). If this occurs *in vivo* during soybean oil biosynthesis, mass spectra of stearate (C18) would show a cytosolic labeling signature similar to the 20 carbon acyl chains. However, the 16 and 18 carbon fatty acids show very similar labeling patterns in both [U-$^{13}C_6$]glucose or [U-$^{13}C_5$]glutamine experiments. We can therefore conclude that 18 carbon saturated fatty acids of soybean oil are not derived from the elongation of 16 carbon precursors in the cytosol.

2.3. Monomers from starch, cell wall, and protein glycans provide information to evaluate glycolytic fluxes in different compartments

Fatty acid labeling can distinguish plastidic from cytosolic acetyl-CoA pools, but provides little insight into the parallel paths of carbohydrate metabolism in the two compartments. This makes it difficult to analyze fluxes through the glycolytic and oxidative pentose phosphate pathways in plant systems. This problem can be addressed in part by comparing the labeling of cell wall and protein glycosylation units that are made in the cytosol with the labeling in glucose monomers of starch, which is made in the plastids. We have therefore used standard cell wall hydrolysis and mass spectrometry protocols and a recently published glucose derivatization technique to garner new labeling data for flux modeling. The comparison of labeling in the different carbohydrate pools is particularly helpful to establish the degree to which sections of metabolism that are duplicated in cytosol and plastid function independently. The answer to this question appears to vary between plant systems (Schwender et al., 2003; Sriram et al., 2004).

2.3.1. Monoacetone derivatives of glucose allow improved labeling analysis in starch

Recently Jin et al. (2004) used the derivatization of glucose to a monoacetone form to increase the labeling infor-

Fragment	Label Expt.	Chain length	M %	M+1 %	M+2 %	M+3 %
C2	[U-^{13}C] glucose	16	70.33(0.90)	5.66(0.07)	24.00(0.83)	
		18	70.00(0.53)	6.00(0.04)	23.99(0.49)	
		20	72.27(1.56)	9.43(0.34)	18.30(1.21)	
		22	72.17(1.79)	9.67(0.53)	18.16(1.27)	
	[U-^{13}C] glutamine	16	90.66(0.59)	2.24(0.15)	7.10(0.45)	
		18	88.77(0.97)	2.79(0.20)	8.43(0.76)	
		20	66.06(0.89)	7.65(0.25)	26.29(1.14)	
		22	66.71(1.57)	7.75(0.13)	25.54(1.70)	
C3	[U-^{13}C] glucose	16	51.68(1.98)	21.34(0.18)	17.60(0.84)	9.38(0.86)
		18	51.05(0.69)	21.82(0.01)	17.19(0.21)	9.95(0.49)
		20	51.69(0.99)	25.84(0.17)	15.84(0.67)	6.62(0.16)
		22	55.42(1.98)	22.99(0.59)	16.02(0.79)	5.58(0.60)
	[U-^{13}C] glutamine	16	80.95(1.06)	11.01(0.53)	6.82(0.47)	1.22(0.06)
		18	79.00(1.62)	11.36(0.76)	8.04(0.92)	1.60(0.06)
		20	59.02(0.94)	14.70(0.29)	22.42(0.82)	3.86(0.41)
		22	49.19(1.41)	22.81(0.21)	18.48(0.28)	9.52(1.34)

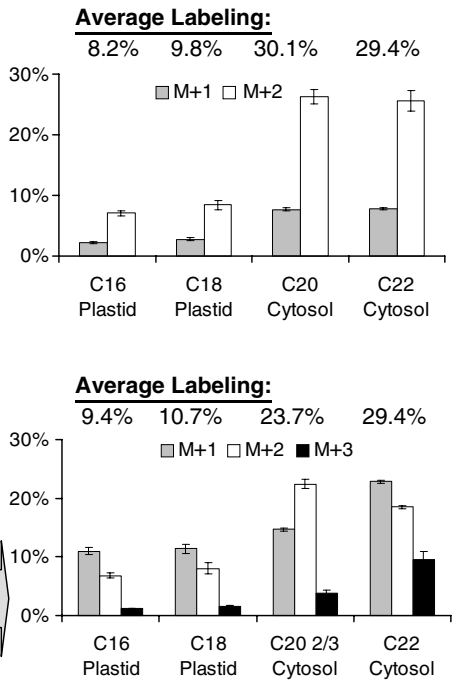

Fig. 4. Isotope incorporation into carboxy-terminal carbons of labeled soybean embryo fatty acids as determined from C2 and C3 McLafferty fragments of butyl amide derivatives of palmitate, stearate, arachidate, and behenate. Standard deviations are given in parenthesis. Histograms to the right present [U-^{13}C]glutamine labeling results for acetyl-CoA building blocks of different compartments. $[M]^+$ is not shown as it is the remaining fraction and is redundant (100%–$[M+1]^+$–$[M+2]^+$–$[M+3]^+$). [U-^{13}C]glutamine results in less label in plastidic acetyl-CoA than cytosolic acetyl-CoA. For chain lengths longer than C18 and in the C3 versus C2 fragment, more carbons of the acyl chain are derived from cytosolic acetyl-CoA and therefore the % label increases as well.

mation obtained from NMR analysis of glucose in a ^{13}C labeling study of hepatic metabolism in rats. Here we have applied a slightly simplified version of this approach to deconvolute ^{13}C NMR spectra of the glucose units of starch after [U-$^{13}C_6$]glucose was provided to soybean embryos developing in culture. The uniform labeling experiment represents a "worst case" scenario from an NMR analytical perspective because it gives the most highly convoluted spectra of glucose. On the other hand providing more highly labeled substrates often results in more metabolite information than singly labeled substrates because the labeling patterns found in downstream metabolites are sensitive to more of the bond breaking and bond forming reactions.

Figs. 5a and 6 show one-dimensional ^{1}H and ^{13}C NMR spectra of glucose obtained from starch using a 500 MHz instrument. A common approach to quantifying positional enrichment for each carbon in the glucose backbone involves first using ^{1}H NMR to determine the absolute enrichment of ^{13}C in the C1 carbon position by comparing the areas of the ^{13}C–H satellite peaks to that of the unlabeled ^{12}C–H peak. For hexoses the proton signals from the C1 hydrogen are the only ones that are sufficiently resolved for label analysis (Fig. 5a). Any errors resulting from this are carried through to the positional enrichment

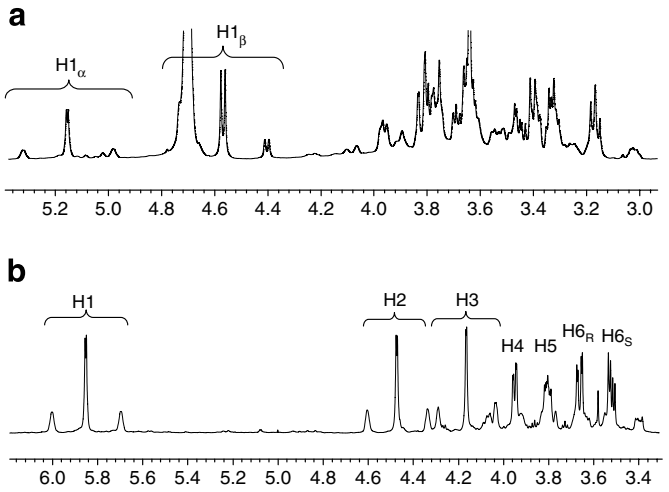

Fig. 5. (a) ^{1}H NMR spectra (500 MHz) of glucose monomers from ^{13}C labeled starch. Quantification of $H1_\alpha$ and/or $H1_\beta$ signals is necessary to obtaining absolute positional enrichments of all carbons. The residual water peak at 4.7 ppm interferes with one ^{13}C satellite for $H1_\beta$. Other proton peaks overlap extensively with one another (b) ^{1}H spectra of monoacetone glucose derived from ^{13}C labeled starch. The H1 and H2 protons along with their ^{13}C satellites are cleanly resolved for both 500 and 600 MHz instruments (600 MHz shown) and can serve independently for calculating the absolute positional ^{13}C enrichments. No alpha and beta conformers are present to complicate the spectrum, making quantitation more straight forward. The H3 signal is also sufficiently resolved for quantifying enrichment.

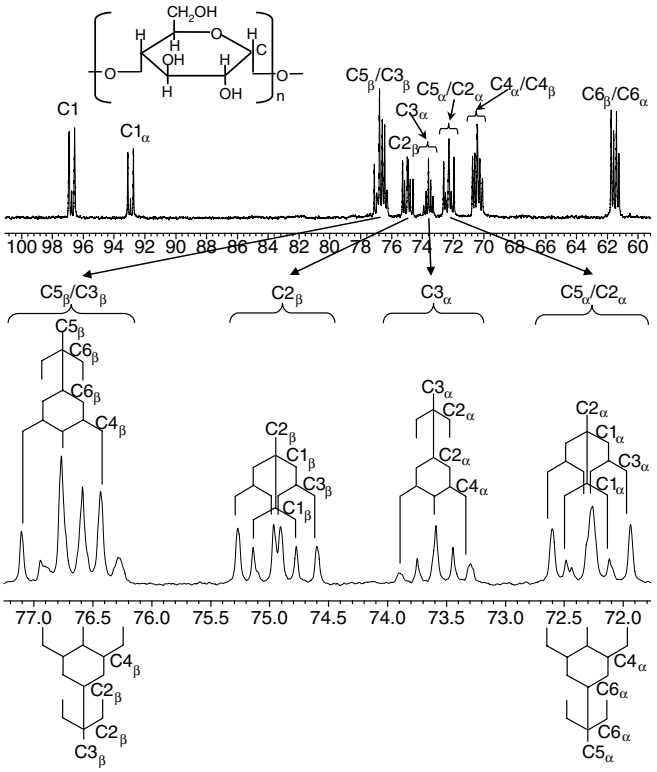

Fig. 6. ^{13}C NMR spectra of starch glucose monomers taken from a glucose labeling experiment with soybean embryos. Part of the spectrum containing carbon peaks that overlap (and which are therefore problematic for bond coupling information) is magnified.

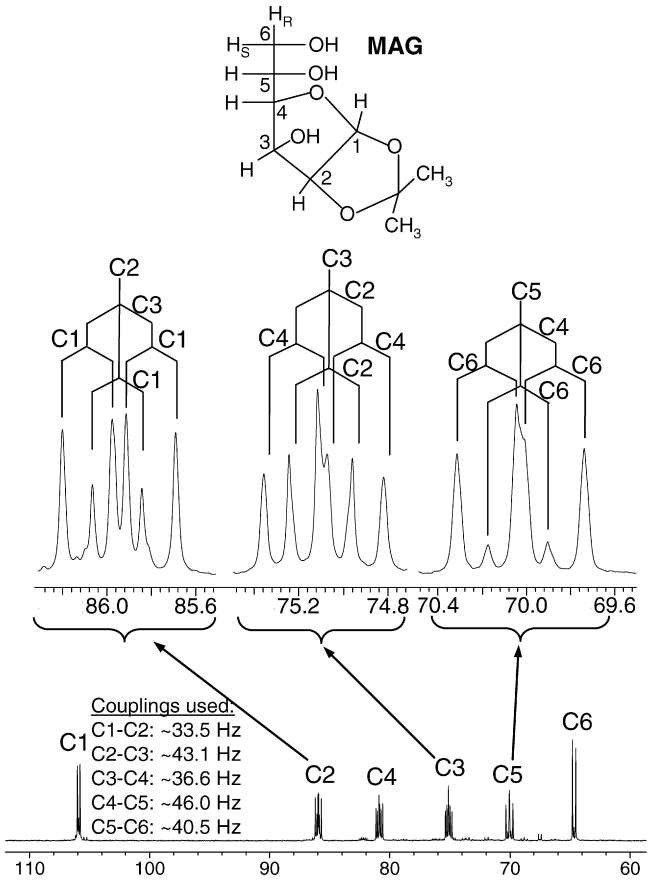

Fig. 7. ^{13}C NMR spectrum for the monoacetone derivative of starch-derived glucose monomers from a ^{13}C labeling experiment one cultured soybean embryos. Expanded subspectra for the signals from C2, C3 and C5 which are poorly resolved in the glucose spectrum are also shown. Bond couplings are more cleanly discernable in the ^{13}C MAG spectrum than in the glucose one.

of all carbons, because the ratio of ^{13}C at C1 to other carbons obtained from the ^{13}C spectrum of the same sample is multiplied by the absolute ^{13}C contents to calculate positional enrichments at each carbon.

The carbon spectrum of labeled glucose is also rather convoluted (Fig. 6). Specifically, the NMR spectrum shows substantial overlap of the $C5_\beta$ with the $C3_\beta$ and the $C5_\alpha$ with the $C2_\alpha$ signals. The result is that positional enrichments are obtainable only from extensive and sometimes successive subtractions of peak intensities from one another, which increases the risks of distortion from contaminants and low signal-to-noise.

Labeling patterns in glucose units of starch has been analyzed by NMR in previous plant metabolic studies (reviewed in Ratcliffe and Shachar-Hill, 2001). While the presence of alpha and beta conformers gives redundant information allowing independent quantification and verification of some peak areas, it also leads to superposition of multiplets and thus more convolution.

Figs. 5b and 7 show the ^{1}H and ^{13}C NMR spectra for glucose units of starch converted to the monoacetone glucose (MAG) derivative. Signals from both the H1 and H2 protons and their ^{13}C-coupled satellites are cleanly resolved in the ^{1}H spectrum, providing measurements of absolute enrichment at two positions. Because for many isotopomer mixtures ^{13}C satellites may be quite small, a contaminant in a satellite would lead to very different conclusions. Having multiple independent confirmations of absolute labeling provides confidence to these important label measurements. As Fig. 5b shows, the H3 proton also has cleanly resolved ^{1}H–^{13}C satellites in spectra for the 600 MHz instrument. (Note: a 500 MHz instrument shows similar abilities to resolve H1 and H2, though H2 and H3 have some overlap in one of each of their satellites.) In the ^{13}C spectrum signals from each of the carbon positions are fully resolved using either 500 or 600 MHz instruments (spectrum of 600 MHz instrument is shown in Fig. 7), making for easy evaluation of positional enrichment by peak integration. Modification of the hexose in this way leads to a more discernable bond connectivity description indicated by the multiplet peak pattern (see insets in Figs. 6 and 7) and more reliable quantitative estimations of ^{13}C–^{13}C bond levels.

2.3.2. Cell wall and protein glycans provide description of cytosolic glycolytic labeling

In most previous studies of plant steady-state fluxes sucrose has been analyzed to provide information on labeling in the important cytosolic pools of hexose phosphates

(e.g. Dieuaide-Noubhani et al., 1997). However, for tissues or conditions where little sucrose is stored or in experiments where sucrose is provided as a substrate and is therefore present in the apoplast and can be taken up intact before being stored in the vacuole (Wink, 1993) the validity of this approach is uncertain. In addition the presence of alternative routes of sucrose synthesis and turnover in plant cells via sucrose synthase, sucrose phosphate synthase, and invertase together with the difficulty in verifying whether complete label equilibration takes place among the various sugar and sugar phosphates in the cytosol make it desirable to have alternative measures of labeling in cytosolic carbohydrates. Analysis of cell wall and protein glycan labeling represent alternative strategies to assess carbon labeling of such cytosolic pools – particularly the key biosynthetic precursor UDP glucose.

Cell wall typically accounts for a large proportion of total plant biomass and its synthesis therefore represents a significant flux in growing cells. In addition, the abundant soybean storage protein, β-conglycinin, undergoes a series of glycosylation steps resulting in 3.8–5.4% carbohydrate by weight (Thanh and Shibasaki, 1978). Sriram et al. (2004) introduced the use of protein glycans as a measure of cytosolic labeling in carbohydrates for flux analysis. Here we employed the hydrolysis of cell wall and protein glycans using trifluoroacetic acid followed by reduction of the carbohydrate monomers and then acetylation to yield the alditol acetate derivatives that can be volatilized and analyzed by GC–MS. Cell wall pectin and hemicellulose can be hydrolyzed into their constituent monomers under acidic conditions and subsequently converted to pentaacetate derivatives (Blakeney et al., 1983; Price, 2004) with or without prior reduction. Detailed labeling information can be obtained by analyzing the alditol acetate derivatives of these monomers using GC–MS. This is examined below along with the effects of reduction prior to derivatization.

The carbohydrate monomers are chromatographically well-resolved with retention times for the alditol acetates of rhamnose (14.9 min), fucose (15.3), arabinose (17.7), xylose (19.7), mannose (22.5), galactose (23.1), and glucose (23.8). Fig. 8 shows the total ion chromatogram for one cell wall component, fucose that was analyzed as fucitol pentaacetate. The postulated breakdown pattern and the molecular weights associated with the remaining fragment are shown (Fig. 8). The identities of the fragments circled in the inset were verified by analyzing the breakdown products of differently labeled standards to confirm the presence or absence of particular backbone carbons in the fragment (see Supplement Table S1 for more labeled standard results). Reduction of the sugars before GC–MS processing, creates symmetry for hexoses that have been converted to alditols and therefore reduces the information content but it confers the benefit of giving only one peak per carbohydrate compound because alpha and beta conformers have been eliminated. This results in more intense signals with improved S/N ratio because two peaks merge into one in the chromatogram. As the alpha/beta conformers

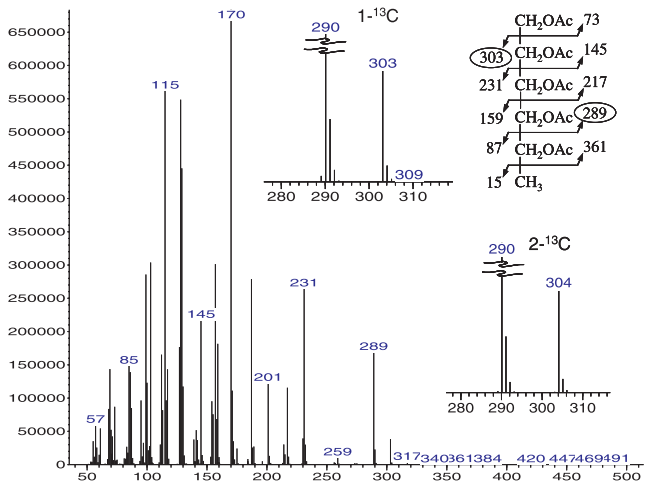

Fig. 8. MS spectrum of fucitol pentaacetate. Inset are subspectra acquired with selected ion monitoring from labeled standards. These were used for fragment identification. The postulated chemical fragmentation pattern with molecular weights of the resulting fragments is also illustrated. A summary of other compounds examined is provided in the Supplement. For fucitol pentaacetate the 1-^{13}C, and 2-^{13}C labeled standards shown (insets) resulted in greater than 99% $[M+1]^+$ ion after correction for natural abundance for the 289 amu (carbons 1–4) product while the ^{12}C unlabeled standard generated 99.9% $[M]^+$ as expected. Similarly, the 1-^{13}C, and 2-^{13}C labeled standards give 100% and 99.6% $[M]^+$ and $[M+1]^+$, respectively, for the 303 amu (carbons 2–6) product and the ^{12}C unlabeled standard also corrects to nearly 100% $[M]^+$ consistent with structural predictions.

are not a reflection of metabolism, but rather post processing, individually they contain no additional information. These advantages/disadvantages must be weighed carefully and will depend upon the amount of material available for analysis, as well as the capabilities of the flux analysis software for handling symmetric label information. Labeling in sugars can also be measured with two-dimensional NMR methods (Shachar-Hill et al., 1996) but spectra of complex mixtures of the sort obtained by hydrolysis of cell walls makes this less straightforward than the GC–MS approach used here.

Table S1 shows that the selected fragments correct well for the presence of natural abundance levels of isotopes in unlabeled samples. Most ^{13}C uniformly labeled hexose standards contain 98–99% ^{13}C, which means that the proportion of completely labeled molecules is approximately $(0.98)^6 = 0.89$; all the measurements are consistent with this isotopic purity. The exception occurs when a symmetric set of fragments that have equivalent weight are generated (e.g. glucose 1234/3456 fragment where [1-$^{13}C_1$]glucose was provided). The fragments have identical molecular weights, but varying degrees of labeling within those weights. In the example above, the first fragment will be completely $[M+1]^+$, while the second fragment that does not contain the first carbon will be entirely unlabeled (i.e. $[M]^+$). The combination of these two fragments results in two different weights together accounting for nearly the entire composition (i.e. $[M+1]^+ + [M]^+ \sim 100\%$, see supplement for more details).

For the pentaacetate derivatization without prior reduction we have also analyzed labeled glucose standards. The derivatives are asymmetric and thus the fragments of interest (verified by the data of Supplement Table S2) yield labeling information from distinct carbon positions. Potentially, if enough material was available, one could pursue in parallel the pentaacetate derivatization, with and without prior reduction to obtain more information. The result of processing without reduction is the generation of two fragments of molecular weights 331 and 317 for glucose containing six and five backbone carbons respectively. Note that one should not apply this finding to other sugars without prior validation, as for example fructose also gives a 317 amu product that is not of the same carbon composition as the glucose fragment (data not shown). Table S2 in the supplement shows data from labeled carbohydrate standards, which are within the label contents specified by the manufacturer of these products (see above).

Figs. 9a and b show comparisons of the labeling patterns in four and five carbon fragments taken from sugar units of starch, cell wall and protein glycan of cultured soybean embryos. Protein glycan is primarily composed of mannose groups and to a lesser extent xylose, glucose and others (Kimura et al., 1997). Here we have primarily used the mannose groups (and for comparative purposes we include galactose) to represent the protein glycan labeling because of their much greater abundance. Since cell wall material is obtained after extracting protein, starch, oil, soluble sugars and acids, we chose not to use data obtained from analyzing the glucose or mannose units after cell wall hydrolysis because of the risks of contamination from residual protein or starch that are predominantly composed of these monomers. We instead focused on monomers that are less susceptible to such contamination, namely rhamnose, and arabinose, but do include galactose, which contributes a further redundant set of measurements to compare cell wall with protein glycan. Fig. 9a shows similar labeling profiles for glycans and cell wall monomers that are made from the same cytosolic UDP-glucose pool. If an underlying contaminant were present, it would significantly alter the label distribution for the corresponding compound making it different from the others, which is not the case. There are differences in the precursor carbon atoms represented in some but not all the different ions measured, which provides additional measurements as well as redundant ones. Xylose and arabinose for example have nearly identical values for all ions. The fragment shown for each in Fig. 9a is the symmetric alditol acetate mixture of carbons one through four and carbons two through five. By contrast the alditol acetates of mannose and galactose give fragments that represent a mixture of carbons one through four and three through six, while the rhamnose fragment is asymmetric and represents carbons one through four. Therefore any differences in mannose and galactose would likely reflect differences in labeling of the cell wall and protein glycans as mannose is the predominant protein glycan while galactose is found in both cell wall and protein glyans. The similarity in labeling profiles between the different fragments shown in Fig. 9b reflects the nearly equivalent positional enrichment at all carbons in these metabolites after labeling soybean embryos with uniformly labeled glucose. Other acceptable four and five carbon fragments that have been verified by 13C carbon standards are detailed in the supplement.

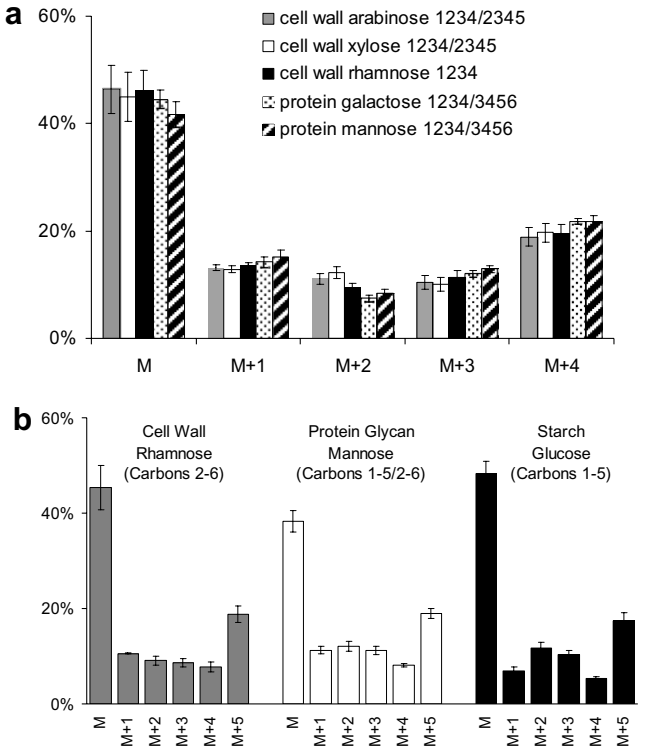

Fig. 9. Comparison of MS peak intensities for selected fragments of cell wall (arabinose, xylose, rhamnose), protein glycan (galactose, mannose) and starch (glucose) monomers, obtained from soybean embryos cultured with [U-13C]glucose. All peaks were corrected for natural abundance. (a) MS data for the four carbon fragment for cell wall and protein glycan (b) Five carbon fragments from cell wall, protein glycan and starch. Rhamnose is an asymmetric molecule and therefore does not give a scrambled carbon result when it is reduced prior to alditol acetate formation. Mannose does result in a symmetric mixture, and starch glucose was not reduced prior to derivatization resulting in slightly different carbon compositions. More fragment data can be found in the Supplementary material.

3. Conclusions

In this work we have investigated methods that can provide increased information on subcellular compartmentation of metabolism. By NMR and GC–MS analysis of monomers from starch, cell wall and protein glycans after ^{13}C labeling of soybean embryo cultures we have identified multiple measurements that distinguish labeling in carbohydrate pools in the cytosol and plastid. Cell wall labeling has not previously been addressed in any flux study to date, though it represents a significant biomass component in plants. Poor label quantitation by NMR for unaltered

carbohydrates is avoided by first derivatizing sugars to their monoacetone counterparts that give clean resolution for positional enrichment information, and provide more bond connectivity information. Additionally, we showed that the GC–MS of long and very long-chain fatty butyl amides derived from triacylglycerols provide more accurate labeling patterns than FAMEs. These patterns serve as signatures of fluxes through acetyl-CoA in the plastid and cytosol and denote the relative contribution of cytosolic elongation to storage triacylglycerols. Together these developments highlight new label measurements, provide more accurate label quantitation, and provide an important source of compartmental data for distinguishing fluxes in different plant cell organelles. Incorporation of a subset of these new measurements into a non-compartmentalized *in silico* study resulted in a 50% increase in information content for the optimal experimental design, suggesting that their addition is equivalent to performing a second labeling experiment (Libourel et al., 2007). It is anticipated that these methods will facilitate fluxomic investigations in multi-organelle systems by providing the compartment-specific data required to improve *in silico* models and our understanding of plant metabolism.

4. Experimental

4.1. Chemicals

Triacylglycerol standards, monosaccharide standards, *n*-butylamine, hexane, pyridine, HCl, were purchased from Sigma–Aldrich (Milwaukee, WI) and all labeled carbohydrate standards were obtained from Isotec, a subsidiary of Sigma–Aldrich at the same location. Acetone and sulfuric acid were purchased from Mallinckrodt Baker (Phillipsburg, NJ) and Fisher (Pittsburgh, PA), respectively. Deuterated solvents for NMR including D_2O and d_3-acetonitrile were purchased from CIL (Andover, MA). Purity of all chemical reagents exceeded 99%.

4.2. Plant material

Soybeans (*Glycine max*) were grown in a greenhouse maintained at 75 F with sunlight supplemented by lamps as necessary to maintain a 15 h day length. Seeds were harvested at the R5 stage representing the early stages of seed expansion (Egli, 2004), surface sterilized with 5% bleach, and rinsed with sterile water. After dissection, embryos (approximately 8 mg dry weight) were incubated in media with sucrose (140 mM), glucose (70 mM), glutamine (35 mM), and asparagine (12.6 mM) as the carbon and nitrogen sources. For the hexose labeling experiment unlabeled glucose was replaced with uniformly labeled glucose resulting in 20% of the total hexose units labeled at all six positions. For the glutamine labeling experiment, [U-^{13}C]glutamine supplanted all unlabeled glutamine but other forms of carbon provided (i.e. sugars and asparagine) remained unlabeled. A revised Linsmaier and Skoog medium originally employed by others (Thompson et al., 1977; Hsu and Obendorf, 1982) supplied necessary salts and the media were also supplemented with Gamborg's vitamins (Sigma, Milwaukee, WI). All cultures were incubated for 14 days with 35 μmol m^{-2} s^{-1} of continuous green light at a temperature of 26–27 °C. Seeds were washed and then sliced into eight pieces, frozen in liquid nitrogen and freeze-dried.

4.3. Oil processing

Oil from seeds was extracted four times by suspending 10 mg (dry weight) of finely ground seed tissue in 2 ml hexane and agitating for 5 min with a stainless steel bead on a MM 301 ball mill shaker (Retsch GmbH, Haan, Germany) at 4000 rpms. After centrifugation at 9300*g* the supernatant was removed and the process repeated. Hexane aliquots were pooled and dried under nitrogen gas at 50 °C and stored at −20 °C until derivatization.

4.4. Butyl amide reactions

Twenty microliters of a 25 μL/mL solution of triolein, tripalmitin, or tristearin standards or soybean oil obtained from 10 mg plant tissue were dissolved in 3 ml hexane and 2 ml *n*-butylamine. Reactions were allowed to proceed for 48 h at 75 °C in a heat block with occasional vortexing. Quenching of the reaction by the addition of 1 mL of 4 M HCl resulted in phase separation of the reactants and partitioning of the unreacted butylamine–HCl to the aqueous phase and amides and unreacted triacylglycerols to the nonpolar solvent phase. The nonpolar hexane phase was concentrated by evaporation under nitrogen before GC–MS analysis.

4.5. GC–MS analysis of butyl amides

A 6850 series gas chromatograph equipped with 5975 MSD and 6850 series auto sampler (Hewlett–Packard, Cincinnati OH) were used for mass spectrometry. Butyl amides were separated using a DB23 column (30 m × 0.2 mm × 0.33 μm). The column was operated with helium-carrier gas and splitless injection (injection temperature 250 °C, detector temperature 280 °C). The temperature profile consisted of 3 min at 100 °C followed by a 10 °C/min ramp to 240 °C, then holding at 240 °C for 4 min, followed by a 2 °C/min ramp to 242 °C, hold for 1 min and a final ramp of 2 °C/min to 250 °C. The EI (70 eV) MS was tuned daily using the *m*/*z* 69, 219 and 502 ions of perfluorotributylamine as a calibrant. Total ion chromatograms were obtained for the mass range of 50–400 amu to determine retention times. Subsequent runs employed selected ion monitoring to quantitatively screen the region of interest between 107 and 135 amu.

Butyl amide standards were made by derivatizing authentic samples of different triacylglycerols and fatty

acids of myristic, palmitic, stearic, oleic, linoleic, linolenic, arachidonic and behenic acids. Results from these standards were compared with a set of butyl amides generously supplied by M. Pollard (Michigan State University). Retention times were assigned accordingly: C14:0 ~ 16.8 min, C16:0 ~ 18.2 min, C18:0 ~ 20.0 min, C18:1 ~ 20.4 min, C18:2 ~ 21.1 min, C18:3 ~ 22.0 min, C20:4 ~ 22.4 min, C22:0 ~ 25.5 min. Fragmentation products were first monitored in full scan mode to identify the C2 and C3 fragment ions (Fig. 2) and to determine the presence of potentially interfering peaks. Labeling was quantified from spectra acquired using selected ion monitoring over the range of molecular weights from 105 to 135 amu. The signals of C2 and C3 fragment ions in spectra of unlabeled C16:0, C18:0 and C18:1 butyl amide derivatives had $[M]^+$, $[M+1]^+$, $[M+2]^+$, and $[M+3]^+$ peak intensities whose proportions were very close to the values expected for unlabeled samples (natural isotopic abundances). The average labeling after correction for natural abundance was always less than 0.5% for the C2 McLafferty fragments and approximately 1.0% for C3 fragments of unlabeled standards. Additionally, monitoring the $[M]^+$ ion indicated that saturation of the detector was not an issue.

4.6. NMR spectroscopy of TAG

^1H NMR and ^{13}C NMR were collected using a Varian (Palo Alto, CA) 500 MHz spectrometer, equipped with 5 mm $^1H/^{13}C$ probes after triacylglycerols were dissolved in 0.7 mL $CDCl_3$. For ^1H spectra an acquisition time of 4.0 s followed by 12 s relaxation time was used and transients were collected for approximately 12 h to ensure sensitive quantitation with a typical spectrum composed of over 1000 scans. For ^{13}C spectra an acquisition time of 1.3 s followed by 20 s relaxation time was used with gated decoupling and transients were collected for approximately 12 h to ensure sensitive quantitation with a typical spectrum composed of ~1500 scans. Adequate relaxation and suppression of nuclear Overhauser effect was verified with unlabeled standards.

4.7. Positional enrichment parameter fitting

As described in the supplement the two butyl amide mass fragments provide more information than is necessary to calculate the positional enrichments, because fatty acids are composed of repeating acetyl-CoA groups with identical labeling if both come from the same source pool. Therefore the isotopomer label description was optimized using a least squares approach with a generalized reduced gradient algorithm provided as the "solver" function on Excel® (Microsoft, Seattle, Washington) and positional enrichments calculated from the optimized isotopomer description.

The least squares approach assumes that the two acetyl-CoA groups that are polymerized to form the three carbon fragment are from the same pool and have identical labeling. In all cases examined here this assumption is validated by the small residual values ($<1\times10^{-3}$ data not shown) from the fitting procedure. In the event that different pools were used to generate the two and three carbon fragments (e.g. fatty acid elongation of plastidic stearate with cytosolic acetyl-CoA to make arachidate) the three carbon fragment would reflect the labeling differences and suitable fitting would be much more difficult. Supplement IV describes the calculated labeling equivalence of the two different fragments.

4.8. Starch, cell wall and glycoprotein glycan processing

As a part of preprocessing to isolate other informative metabolites, oil, free amino acids, organic acids, protein and other water and salt soluble components were preferentially removed according to standard methods (Yazdi-Samadi et al., 1977; Schwender and Ohlrogge, 2002; Alonso et al., 2005). Starch was prepared by first autoclaving for 1hr the previously extracted pellet in the presence of 0.5 mL of 0.1 M acetate buffer pH 4.8. After cooling to room temperature a 10 mg solution of amyloglucosidase/amylase (Sigma, Milwaukee, WI) was added, vortexed and incubated for 1 h at 55 °C. After enzyme denaturation and removal by adding 1 ml ethanol, heating to 95 °C for 15 min and spinning for 5 min at 4000 rpms, the starch fraction in the supernatant was removed. The pellet was extracted again with 2.5 mL 80% ethanol and the fractions were pooled, dried, and stored at −20 °C until derivatization.

After starch extraction, the remaining material is largely composed of cell wall pectins, hemicellulose, and cellulose. This fraction was treated with 500 μL 2 N trifluoroacetic acid for 2 h at 120 °C. Samples were spun at 4000 rpms and the supernatant containing hydrolyzed sugars was resuspended in 500 μL of NH_4OH 0.5 M and dried under nitrogen to neutralize the samples, which were then stored until further derivatization (Blakeney et al., 1983). Proteins that were previously extracted were identically hydrolyzed with TFA to obtain the mannose-rich protein glycan fraction.

4.9. MAG sample preparation

Hydrolyzed starch in the form of glucose (~5 mg) was dissolved in 3 mL acetone with the pH reduced to ~1 by addition of 4 M sulfuric acid and shaken on an oscillatory shaker for 4 h at room temperature. After 1 min centrifugation at 4000 rpms supernatant was removed by filtration or decanting and 2 ml H_2O along with 3 M Na_2CO_3 was added until the pH was 2.0. At pH 2 the solution was agitated on an orbital shaker overnight. Next the pH was adjusted to 8.0 with 3.0 M Na_2CO_3 and dried under nitrogen and minimal heating at 50 °C. Next the MAG was preferentially extracted from other components by the addition of hot ethyl acetate (5 ml). The acetate soluble fraction was removed after centrifugation for 1 min at 4000 rpms and dried as before.

4.10. NMR spectroscopy of MAG

^{1}H NMR and ^{13}C NMR were collected using Varian (Palo Alto, CA) 500 MHz and 600 MHz Inova spectrometers equipped with 5 mm $^{1}H/^{13}C$ probes after MAG was dissolved in a solution of 90% d_3-acetonitrile/10% D_2O. For ^{13}C spectra an acquisition time of 1.3 s followed by 20 s relaxation time was used and transients were collected for approximately 12 h to ensure sensitive quantitation with a typical spectrum composed of ~1500 scans. Jin et al. (2004) report T1 values of less than 4 s for all of the carbons of interest (excluding the carbons derived from acetone), therefore we used a 20 s delay (5 times T1) for adequate relaxation and gated decoupling of the ^{13}C spectra to avoid distortion due to the nuclear Overhauser effect. Absence of distortion was confirmed with unlabeled standards. For ^{1}H spectra an acquisition time of 4.0 s followed by 20 s relaxation time was used and transients were collected for approximately 12 h to ensure sensitive quantitation with a typical spectrum composed of over 1000 scans.

4.11. Alditol acetate derivatization

For GC–MS analysis, hexoses were derivatized to alditol acetates with or without prior reduction. Carbohydrates were suspended in 150 μL of NH_4OH 2 M, and reduced by addition of 3 mL of $NaBH_4$ (50 mg/mL) in NH_4OH 2 M for 1.5 h at 40 °C. The reduction was terminated by careful addition of 100 μL of concentrated acetic acid. Next samples were dried and resuspended in 500 μL of acid acetic/MeOH (1/9 v:v) by vigorous vortexing and again dried under N_2 while heating to 40 °C. After acidification, 600 μL of 1-methyl-imidazole was added and the samples were resuspended by vortexing, then 2 mL of acetic anhydride was added and the reaction allowed to proceed for 30 min. After termination by drop-wise addition of the solution into 4 mL of water, the contents were allowed to cool and thrice extracted with methylene chloride (1 mL each time) followed by at least one back extraction with water. The methylene chloride fraction was analyzed by GC–MS.

4.12. GC–MS of alditol acetates

A 6850 series gas chromatograph equipped with 5975 MSD and 6850 series auto sampler (Hewlett–Packard, Cincinnati OH) were used for diagnostic evaluation of products. Alditol acetates were separated using a SP2330 column (30 m × 0.2 mm × 0.33 μm). The column was operated with helium-carrier gas and splitless injection (injection temp 250 °C, detector temp 280 °C). A temperature profile that included 1 min at 150 °C followed by a 5 °C/min ramp to 175 °C, followed by a 4 °C/min ramp to 240 °C, and a final ramp of 10 °C/min to 250 °C was employed to separate and sequentially elute the products. Perfluorotributylamine served as a calibrant for the EI (70 eV) MS that was tuned daily using m/z 69, 219 and 502 ions. Initially total ion chromatograms were obtained for the mass range of 50–400 amu to determine retention times for derivatized standards of: rhamnose (~14.9 min), arabinose (~17.7 min), xylose (~19.7 min), mannose (~22.4 min), galactose (~23.1 min) and glucose (~23.8 min). Subsequent runs employed selected ion monitoring to quantitatively screen the region of interest between 285 and 310 amu.

Acknowledgements

We thank Drs. Mike Pollard, Dan Jones, Jorg Schwender, Ana Alonso and Igor Libourel for helpful discussions, the Michigan Soy Promotion Committee and the Biotechnology Research and Development Corporation for partial funding support of this work. We thank the MSU Max T. Rogers NMR Facility and the MSU Mass Spectrometry Facility for equipment used and Dr. Daniel Holmes and Mrs. Beverly Chamberlin for technical advice on spectroscopic data acquisition. Additionally the authors thank the editors and anonymous reviewers for helpful comments and suggestions that have improved the manuscript.

Appendix A. Supplementary data

Supplementary data associated with this article can be found, in the online version, at doi:10.1016/j.phytochem.2007.04.010.

References

Aiba, S., Matsuoka, M., 1979. Identification of metabolic model: citrate production from glucose by *Candida lipolytica*. Biotechnol. Bioeng. 21, 1373–1386.

Alonso, A.P., Vigeolas, H., Raymond, P., Rolin, D., Dieuaide-Noubhani, M., 2005. A new substrate cycle in plants. Evidence for a high glucose-phosphate-to-glucose turnover from *in vivo* steady-state and pulse labeling experiments with [C-13] glucose and [C-14] glucose. Plant Physiol. 138, 2220–2232.

Antoniewicz, M.R., Kelleher, J.K., Stephanopoulos, G., 2007. Elementary metabolite units (EMU): a novel framework for modeling isotopic distributions. Metab. Eng. 9, 68–86.

Bao, X.M., Pollard, M., Ohlrogge, J., 1998. The biosynthesis of erucic acid in developing embryos of *Brassica rapa*. Plant Physiol. 118, 183–190.

Bao, X., Focke, M., Pollard, M., Ohlrogge, J., 2000. Understanding *in vivo* carbon precursor supply for fatty acid synthesis in leaf tissue. Plant J. 22, 39–50.

Barrett, P.B., Harwood, J.L., 1998. Characterization of fatty acid elongase enzymes from germinating pea seeds. Phytochemistry 48, 1295–1304.

Blakeney, A.B., Harris, P.J., Henry, R.J., Stone, B.A., 1983. A simple and rapid preparation of alditol acetates for monosaccharide analysis. Carbohydr. Res. 113, 291–299.

Bolton, P., Harwood, J.L., 1977. Fatty acid biosynthesis by a particulate preparation from germinating pea. Biochem. J. 168, 261–269.

Christie, W.W., 2003. Lipid Analysis. The Oily Press, Bridgwater, England.

Coates, S.W., Gurney Jr., T., Sommers, L.W., Yeh, M., Hirschberg, C.B., 1980. Subcellular localization of sugar nucleotide synthetases. J. Biol. Chem. 255, 9225–9229.

daSilva, P.M.F.R., Eastmond, P.J., Hill, L.M., Smith, A.M., Rawsthorne, S., 1997. Starch metabolism in developing embryos of oilseed rape. Planta 203, 480–487.

Dauner, M., Sauer, U., 2000. GC–MS analysis of amino acids rapidly provides rich information for isotopomer balancing. Biotechnol. Prog. 16, 642–649.

Dieuaide-Noubhani, M., Canioni, P., Raymond, P., 1997. Sugar-starvation-induced changes of carbon metabolism in excised maize root tips. Plant Physiol. 115, 1505–1513.

Egli, D.B., 2004. Seed-fill duration and yield of grain crops. Adv. Agron. 83, 243–271.

Ettenhuber, C., Spielbauer, G., Margl, L., Hannah, L.C., Gierl, A., Bacher, A., Genschel, U., Eisenreich, W., 2005. Changes in flux pattern of the central carbohydrate metabolism during kernel development in maize. Phytochemistry 66, 2632–2642.

Ettenhuber, C., Radykewicz, T., Kofer, W., Koop, H.U., Bacher, A., Eisenreich, W., 2006. Metabolic flux analysis in complex isotopolog space. Recycling of glucose in tobacco plants. Phytochemistry 66, 323–335.

Fagerquist, C.K., Schwarz, J.M., 1998. Gas phase acid–base chemistry and its effects on mass isotopomer abundance measurements of biomolecular ions. J. Mass Spectrom. 33, 144–153.

Fagerquist, C.K., Neese, R.A., Hellerstein, M.K., 1999. Molecular ion fragmentation and its effects on mass isotopomer abundances of fatty acid methyl esters ionized by electron impact. J. Am. Soc. Mass Spectrom. 10, 430–439.

Fagerquist, C.K., Hellerstein, M.K., Faubert, D., Bertrand, M.J., 2001. Elimination of the concentration dependence in mass isotopomer abundance mass spectrometry of methyl palmitate using metastable atom bombardment. J. Am. Soc. Mass Spectrom. 12, 754–761.

Feingold, D.s., Avigad, G., 1980. Sugar nucleotide transformation in plants. In: Stumpf, P.K., Conn, E.E. (Eds.), . In: The Biochemistry of Plants: A Comprehensive Treatise, vol. 3. Academic Press, New York, pp. 101–170.

Follstad, B.D., Stephanopoulos, G., 1998. Effect of reversible reactions on isotope label distributions. Analysis of the pentose phosphate pathway. Eur. J. Biochem. 252, 360–372.

Hellerstein, M.K., Neese, R.A., 1999. Mass isotopomer distribution analysis at eight years: theoretical, analytic, and experimental considerations. Am. J. Physiol. 276, E1146–E1170.

Hsu, F.C., Obendorf, R.L., 1982. Compositional analysis of *in vitro* matured soybean seeds. Plant Sci. Lett. 27, 129–135.

Jin, E.S., Jones, J.G., Merritt, M., Burgess, S.C., Malloy, C.R., Sherry, A.D., 2004. Glucose production, gluconeogenesis, and hepatic tricarboxylic acid cycle fluxes measured by nuclear magnetic resonance analysis of a single glucose derivative. Anal. Biochem. 327, 149–155.

Kimura, Y., Ohno, A., Takagi, S., 1997. Structural analysis of N-glycans of storage glycoproteins in soybean (*Glycine max*. L) seed. Biosci. Biotech. Biochem. 61, 1866–1871.

Klapa, M.I., Aon, J.C., Stephanopoulos, G., 2003. Systematic quantification of complex metabolic flux networks using stable isotopes and mass spectrometry. Eur. J. Biochem. 270, 3525–3542.

Kopka, J., Ohlrogge, J.B., Jaworski, J.G., 1995. Analysis of *in vivo* levels of acyl-thioesters with gas chromatography/mass spectrometry of the butyl amide derivative. Anal. Biochem. 224, 51–60.

Lange, B.M., Ghassemian, M., 2005. Comprehensive post-genomic data analysis approaches integrating biochemical pathway maps. Phytochemistry 66, 413–431.

Libourel, I.G.L., Gehan, J.P., Shachar-Hill, Y., 2007. Design of substrate label for steady state flux measurements in plant systems using the metabolic network of *Brassica napus* embryos. Phytochemistry, doi:10.1016/j.phytochem.2007.04.033.

McLafferty, F.R., 1959. Mass spectrometric analysis – molecular rearrangements. Anal. Chem. 31, 82–87.

Morgan, J., Rhodes, D., 2002. Mathematical modeling of plant metabolic pathways. Metab. Eng. 4, 80–89.

Patterson, B.W., Wolfe, R.R., 1993. Concentration-dependence of methyl palmitate isotope ratios by electron-impact ionization gas-chromatography mass-spectrometry. Biol. Mass Spectrom. 22, 481–486.

Price, N.P.J., 2004. Acyclic sugar derivatives for GC/MS analysis of C-13-enrichment during carbohydrate metabolism. Anal. Chem. 76, 6566–6574.

Ratcliffe, R.G., Shachar-Hill, Y., 2001. Probing plant metabolism with NMR. Ann. Rev. Plant Biol. 52, 499–526.

Ratcliffe, R.G., Shachar-Hill, Y., 2006. Measuring multiple fluxes through plant metabolic networks. Plant J. 45, 490–511.

Rontein, D., Dieuaide-Noubhani, M., Dufourc, E.J., Raymond, P., Rolin, D., 2002. The metabolic architecture of plant cells – stability of central metabolism and flexibility of anabolic pathways during the growth cycle of tomato cells. J. Biol. Chem. 277, 43948–43960.

Ryhage, R., Stenhange, E., 1963. In: McLafferty, F.W. (Ed.), Mass Spectrometry of Organic Ions. Academic Press, New York, pp. 399–452.

Schmidt, K., Carlsen, M., Nielsen, J., Villadsen, J., 1997. Modeling isotopomer distributions in biochemical networks using isotopomer mapping matrices. Biotechnol. Bioeng. 55, 831–840.

Schwender, J., Ohlrogge, J.B., 2002. Probing *in vivo* metabolism by stable isotope labeling of storage lipids and proteins in developing *Brassica napus* embryos. Plant Physiol. 130, 347–361.

Schwender, J., Ohlrogge, J.B., Shachar-Hill, Y., 2003. A flux model of glycolysis and the oxidative pentose phosphate pathway in developing *Brassica napus* embryos. J. Biol. Chem. 278, 29442–29453.

Schwender, J., Goffman, F., Ohlrogge, J.B., Shachar-Hill, Y., 2004. Rubisco without the Calvin cycle improves the carbon efficiency of developing green seeds. Nature 432, 779–782.

Schwender, J., Shachar-Hill, Y., Ohlrogge, J., 2006. Mitochondrial metabolism in developing embryos of *Brassica napus*. J. Biol. Chem. 281, 34040–34047.

Shachar-Hill, Y., Pfeffer, P.E., Germann, M.W., 1996. Following 13-C and 15-N labeling in plant metabolism with heteronuclear two-dimensional NMR spectroscopy. Anal. Biochem. 110, 110–118.

Smith, A.M., Martin, C., 1993. Starch biosynthesis and the potential for its manipulation. In: Grierson, D. (Ed.), Plant Biotechnology, Biosynthesis and Manipulation of Plant Products, vol. 3. Blackie and Son, Glasgow, pp. 1–54.

Spielbauer, G., Margl, L., Hannah, L.C., Romisch, W., Ettenhuber, C., Bacher, A., Gierl, A., Eisenreich, W., Genschel, U., 2006. Robustness of central carbohydrate metabolism in developing maize kernels. Phytochemistry 67, 1460–1475.

Sriram, G., Fulton, D.B., Iyer, W., Peterson, J.M., Zhou, R.L., Westgate, R.E., Spalding, M.H., Shanks, J.V., 2004. Quantification of compartmented metabolic fluxes in developing soybean embryos by employing biosynthetically directed fractional C-13 labeling, [C-13, H-1] two-dimensional nuclear magnetic resonance, and comprehensive isotopomer balancing. Plant Physiol. 136, 3043–3057.

Stephanopoulos, G., Aristodou, A., Nielsen, J., 1998. Metabolic Engineering: Principles and Methodologies. Academic Press, San Diego.

Szyperski, T., 1995. Biosynthetically directed fractional ^{13}C-labeling of proteinogenic amino acids an efficient analytical tool to investigate intermediary metabolism. Eur. J. Biochem. 232, 433–448.

Szyperski, T., 1998. ^{13}C-NMR, MS and metabolic flux balancing in biotechnology research. Quart. Rev. Biophys. 31, 41–106.

Takayama, M., 1995. Metastable McLafferty rearrangement reaction in the electron impact ionization of stearic acid methyl ester. Int. J. Mass Spectrom. Ion Proc. 144, 199–204.

Thanh, V.H., Shibasaki, K., 1978. Major proteins of soybean seeds. Subunit structure of β-conglycinin. J. Agric. Food Chem. 26, 692–695.

Thompson, J.F., Madison, J.T., Muenster, A.E., 1977. In vitro culture of immature cotyledons of soya bean (*Glycine max* L. Merr.). Ann. Bot. 41, 29–39.

Tulloch, A.P., Hogge, L.R., 1985. Investigation of the formation of MH+ and other ions in the mass spectrum of methyl decanoate using specifically deuterated decanoates. Chem. Phys. Lipids 37, 271–281.

van der Heijden, R.T.J.M., Romein, B., Heijnen, J.J., Hellinga, C., Luyben, K.C.A.M., 1994. Linear constraint relations in biochemical reaction systems. 1. Classification of the calculability and the balanceability of conversion rates. Biotechnol. Bioeng. 43, 3–10.

van Winden, W.A., van Dam, J.C., Ras, C., Kleijn, R.J., Vinke, J.L., van Gulik, W.M., Heijnen, J.J., 2005. Metabolic-flux analysis of *Saccharomyces cerevisiae* CEN.PK113-7D based on mass isotopomer measurements of ^{13}C-labeled primary metabolites. FEMS Yeast Res. 5, 559–568.

Varma, A., Boesch, B.W., Palsson, B.O., 1993a. Stoichiometric interpretation of *Escherichia coli* glucose catabolism under various oxygenation rates. Appl. Environ. Microbiol. 59, 2465–2473.

Varma, A., Boesch, B.W., Palsson, B.O., 1993b. Biochemical production capabilities of *Escherichia coli*. Biotechnol. Bioeng. 42, 59–73.

Walter-Heldt, H., 2005. Polysaccharides are storage and transport forms of carbohydrates produced by photosynthesis. In: Walter-Heldt, H. (Ed.), Plant Biochemistry, third ed. Academic Press, New York, pp. 243–273.

Wiechert, W., Mollney, M., Petersen, S., deGraaf, A.A., 2001. A universal framework for ^{13}C metabolic flux analysis. Metab. Eng. 3, 265–283.

Wink, M., 1993. The plant vacuole – a multifunctional compartment. J. Exp. Bot. 44 (Suppl. S), 231–246.

Wittmann, C., Heinzle, E., 1999. Mass spectrometry for metabolic flux analysis. Biotech. Bioeng. 62, 739–750.

Yazdi-Samadi, B., Rinne, R.W., Seif, R.D., 1977. Components of developing soybean seeds: oil, protein, sugars, starch, organic acids, and amino acids. Agron. J. 69, 481–486.

Zamboni, N., Fischer, E., Sauer, U., 2005. FiatFlux – a software for metabolic flux analysis from ^{13}C-glucose experiments. BMC Bioinform. 6, 209.

Zupke, C., Stephanopoulos, G., 1994. Modeling of isotope distributions and intracellular fluxes in metabolic networks using atom mapping matrices. Biotechnol. Prog. 10, 489–498.